31st Annual International Conference of the IEEE EMBS
Minneapolis, Minnesota, USA, September 2-6, 2009

Automated Detection of Asynchrony in Patient-Ventilator Interaction

Qestra Mulqueeny, *Student Member, IEEE*, Stephen J. Redmond, *Member, IEEE* , Didier Tassaux, Laurence Vignaux, Philippe Jolliet, Piero Ceriana, Stefano Nava, Klaus Schindhelm, Nigel H. Lovell, *Senior Member, IEEE*

***Abstract*—An automated classification algorithm for the detection of expiratory ineffective efforts in patient-ventilator interaction is developed and validated. Using this algorithm, 5624 breaths from 23 patients in a pulmonary ward were examined. The participants (N=23) underwent both conventional and non-invasive ventilation. Tracings of patient flow, pressure at the airway, and transdiaphragmatic pressure were manually labeled by an expert. Overall accuracy of 94.5% was achieved with sensitivity 58.7% and specificity 98.7%. The results demonstrate the viability of using pattern classification techniques to automatically detect the presence of asynchrony between a patient and their ventilator.**

I. Introduction

ENSURING quality interaction between a patient and their ventilator is critical to minimize the work of breathing of the patient. Increased work of breathing caused by patient-ventilator asynchrony is associated with negative patient outcomes and has been shown to be highly prevalent; studies have shown up to 43% of patients suffer severe asynchrony [1].

With proper supervision and adjustment of ventilator settings, asynchrony may be mitigated by the clinician. However, monitoring asynchrony is a challenge. Knowledge of its existence firstly requires high resolution and real-time display of airway pressure delivered by the ventilator, the patient's airflow and a measure of inspiratory activity, such as diaphragmatic electromyogram (EMGdi) or esophageal pressure, measured invasively via a balloon catheter. Furthermore, expert visual interpretation of these signals is critical to diagnose the quality of patient-ventilator interaction.

Attempts to automate this process have been few and have either not taken a pattern classification approach or have used very few morphologically-based features [2, 3].

Q. Mulqueeny, and K. Schindhelm are with ResMed Pty Ltd, and the Graduate School of Biomedical Engineering, University of New South Wales, Sydney NSW 2052, Australia. N.H. Lovell (email: N.Lovell@unsw.edu.au) and S. J. Redmond, are with the Graduate School of Biomedical Engineering, University of New South Wales, Sydney NSW 2052, Australia. P. Ceriana and S. Nava are with the Respiratory Intensive Care Unit, Fondazione S. Maugeri, Instituto Scientifico di Pavia, Via Ferrata 8 27100 Pavia, Italy. D. Tassaux, L. Vignaux and P. Jolliet are with the University Hospital, Intensive Care, 1211 Geneva 14, Switzerland. The authors would like to thank Fondazione S. Maugeri, for the provision of data.

One of the common and physiologically significant types of patient-ventilator asynchrony is the presence of ineffective patient efforts occurring during the expiratory phase: the 'expiratory ineffective effort' (eIE). Occurring mainly in obstructive patients, these are often caused by intrinsic positive-end-expiratory pressure (PEEPi), which acts as an inspiratory threshold load that the respiratory muscles cannot overcome, thus resulting in an inability to systematically trigger the ventilator.

This paper reviews a cohort of signals describing patient-ventilator interaction in 23 subjects acquired from an existing database, all recorded in a respiratory unit (Fondazione S. Maugeri, Pavia, Italy). It furthermore describes an approach for algorithmically detecting the prevalence of eIEs on a breath-by-breath basis. Such a method, for monitoring this kind of patient-ventilator asynchrony, is of critical advantage in clinical decision-making procedure to reduce the work of breathing and increase efficacy of treatment, for patients benefitting from ventilatory support.

II. Methods

A. Database

Data from 23 subjects were drawn from an existing database at the pulmonology unit at the Maugeri Institute, Pavia, Italy. Patients had either undergone non-invasive ventilation after recovering from acute respiratory failure, or had received conventional ventilation in the advanced stage of weaning. For each subject, between 10-20 minutes of respiratory data was obtained consisting of the following tracings. Flow at the airway opening was measured with a heated pneumotachograph (Hans-Rudolf 3700, Kansas, USA) and a differential pressure transducer (Honeywell ± 300 cm H_2O; Freeport IL, USA) placed between the mask and the Y-piece of the ventilator, or at the Y-piece. Airway pressure (Pao) was measured from a side port between the pneumotachograph and the face mask, or the endotracheal tube. Esophageal and gastric pressures were measured with a balloon-catheter system. To this end, an esophageal balloon was positioned at the lower third of the esophagus, filled with 0.5 ml of air and a gastric balloon filled with 1 ml of air. The proper position of the balloon was verified using the occlusion test. Transdiaphragmatic pressure (Pdi) was calculated as the difference between gastric (Pga) and esophageal (Pes) pressures.

B. Breath Segmentation Algorithm

A segmentation algorithm was applied to the data to demark each breath instance. A state-machine consisting of four states and operating on the flow and volume signals identified the points in time at the beginning and end of each inspiration, correspondingly when the state machine enters the *Confirmed Inspiration* and the *Confirmed Expiration* states (Fig. 1). Flow and volume thresholds expressed in the state diagram logic expressions are $\alpha = 0.05$ L/s and β=150 mL.

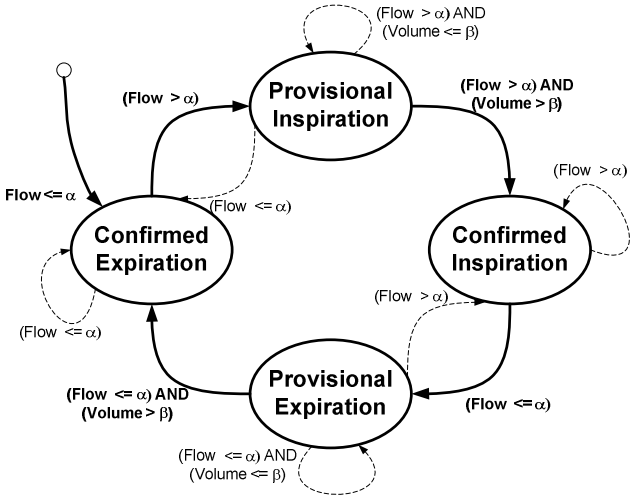

Fig.1. Breath segmentation state diagram.

C. Visual Asynchrony Scoring

Visual scoring of asynchronies and correction of breath demarcation was carried out by a single physician specialized in mechanical ventilation using a custom designed graphical user interface (Matlab, MathWorks Inc., USA). The physician was blinded to the clinical data of the patient and was not involved in their care. The beginning of inspiration was globally adjusted for each patient by 200 ms (±50 ms) to align with the deflection of Pdi to correspond with the initiation of patient effort. Subsequently, breaths were labeled as containing an eIE if a positive Pdi tidal swing occurred during expiration, but was not followed by inspiratory support from the ventilator (Fig. 2).

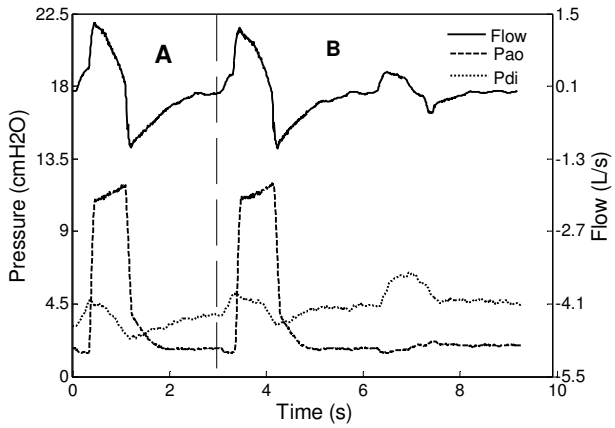

Fig. 2. Shows flow, airway pressure (Pao) and transdiaphragmatic pressure (Pdi) for normal breath (A) and breath with an eIE (B). Positive swings in Pdi indicate inspiratory effort by the patient. Note, B is characterized predominantly by a perturbation on the flow signal during mid-expiration.

A total of 5624 breaths were analyzed and labeled as summarized in Table I.

TABLE I. SUMMARY OF BREATH LABELS BY HUMAN EXPERT

Category	Count	% of Total
Expiratory Ineffective Effort	567	10.1
Other	5057	89.9
Physical breaths	5624	100

D. Feature Selection

As the goal of this study was to automate the detection of asynchronies via non-invasive and simple means, features were derived using only flow and Pao and not from Pdi. The following features were derived for each breath and are summarized in Table II:

Physiologically based features:
RR_{breath} = $1/T_{breath}$, the respiratory rate pertaining to the particular breath calculated as the inverse of the period; *RR ratio* = RR_{breath}/RR_{mean}, the ratio of the respiratory rate of the breath to the mean respiratory rate calculated over 5 minutes; *IE ratio* = T_i/T_{breath}, the ratio of inspiratory time to the period of the breath; Vol_I – absolute volume inhaled (the integral of the flow during inspiration); Vol_E – absolute volume exhaled (the integral of the flow during expiration); *breathLeak* = Vol_I - Vol_E, the volume leaked between inspiration and expiration; *Vol ratio* = Vol_I / Vol_E, the ratio of inspiratory to expiratory volumes.

Respiratory mechanics based features:
Mechanics parameters were calculated for both inspiratory and expiratory phases (denoted by subscript *i* and *e* respectively) of each breath by a multiple linear regression fit of the pressure, flow and volume data to the first order single compartment lung model:

$$Pao = (Flow)(R) + \frac{Vol}{C} + PEEPtot$$

where *PEEPtot* is the sum of the applied pressure during expiration and the patient's intrinsic PEEP, *R* is the resistance of the respiratory system, and *C* is the compliance of the respiratory system. $\tau = RC$, is the patient's time constant.

Expiratory flow morphology based features:
Often asynchronies are characterized by irregularities or perturbations on the pressure and flow signals. As the signal-to-noise ratio of these irregularities is generally higher on the flow signal than the pressure, flow was used as the main signal for deriving the feature set. To identify these irregularities during expiration, the goal was to derive significant deviations of the flow curve from an approximated 'normal' expiratory shape. A segmented moving average filter with time constant 0.1 s was applied to the flow signal separately for each respiratory phase. For each period of expiration, the location of the maximum expiratory flow occurring in the first 25% of expiration was obtained.

TABLE II. FEATURE LIST

1	RR breath	Respiratory Rate based features
2	RR ratio	
3	IE ratio	
4	Vol_I	Volume based features
5	Vol_E	
6	breathLeak	
7	Vol ratio	
8	$PEEPi_i$	Respiratory Mechanics based features
9	R_i	
10	C_i	
11	τ_i	
12	$PEEPi_e$	
13	R_e	
14	C_e	
15	τ_e	
16	InterpMinima	Expiratory Flow Morphology based features
17	InterpMinima-2/3	
18	PW linear approx power	
19	PW vol deviation	
20	PW dist flow maxmin	
21	PW distance ratio	

interpMinima - for the remainder of expiration, local minima were obtained at intervals of 150ms. Interpolation from these minima for the duration of expiration was made. The result was used to de-trend the moving average by subtraction, and the power (RMS) was obtained for the resultant signal,

interpMinima-2/3 – using the de-trended interpolated minima signal above, the power (RMS) was calculated for the last two thirds of expiration.

PW linear approx power - a piecewise bilinear approximation was made for the remainder of expiration after the location of maximum expiratory flow. The second linear component was used to de-trend the moving average by subtraction. The power (RMS) was obtained for the resultant signal.

PW vol deviation – the integral of the rectified and de-trended moving average (via subtraction of the piecewise linear approximation) was calculated.

PW dist flow maxmin – the indices of the minimum and maximum de-trended moving average (via subtraction of the piecewise linear approximation) were obtained. These were used to locate the corresponding real flow values in the moving average expiratory flow signal. The amplitude distance between them was calculated.

PW distance ratio – the *PW dist flow maxmin* taken as a fraction of the distance between the maximum flow point (calculated previously) and the peak expiratory flow.

Morphological features were normalized across their mode value for each patient.

E. Classifier Model: Parzen Window Estimation

After the features were extracted from the signals, each breath had an associated feature vector, **x**, containing up to 21 features for this application. To design the classifier, Bayes' rule was used to find the class for a given test feature vector that maximized the posterior probability

$$P(\omega_i \mid \mathbf{x}) = \frac{P(\omega_i)\, p(\mathbf{x} \mid \omega_i)}{p(\mathbf{x})} \quad , \qquad (1)$$

where ω_i signifies the *i*th class.

A Parzen window classifier is utilized for classification. The window type was chosen as a Gaussian radial basis function (RBF):

$$\phi_I(\mathbf{x}) = \frac{1}{(2\pi)^{\frac{d}{2}} r^d} \exp\left(\frac{\left\| \mathbf{x} - \mathbf{x}_i \right\|^2}{r^2} \right), \qquad (2)$$

where $\mathbf{x}$ is a feature vector extracted from an unknown breath, which must be classified, and $\mathbf{x}_i$ represents a feature vector contained in the training set database. r was calculated as the median of the Euclidean distances between all feature vectors in the training set.

$\omega \in \{B_1, B_2\}$ represented the class labels for each of our two breath classes. For each breath class, the discriminant function was evaluated:

$$g_\omega(\mathbf{x}) = \sum_{i \in \xi} \phi_i(\mathbf{x}) \ , \qquad (3)$$

where $\xi \subset \{1,...N\}$ is the set of indices of the feature vectors in the training set labelled as belonging to class ω.

A classification result, $\omega_{\mathbf{x}}$, was obtained as:

$$\omega_{\mathbf{x}} = \arg\max_{\omega} \{ g_\omega(\mathbf{x}) \}; \qquad (4)$$

that is the class, $\omega \in \{B_1, B_2\}$, which maximizes Eq.3.

F. Feature Subset Selection

A form of the sequential forward floating search (SFSS) algorithm was exploited to identify the feature subset that maximizes the classification performance criterion [4], in this case the accuracy of breaths correctly classified. Three passes of the sequential forward selection (SFS) algorithm are made to choose up to the first three features that contribute the greatest improvement to performance. A backwards pass is then made to check if removing any features one at a time improves performance. Forward and backwards passes then alternate to add or trim features until performance is maximized.

G. Cross-fold Validation

To validate the classifier, features from all but one patient formed the training data for the classifier, which was subsequently tested on features from the withheld patient. This procedure of withholding a patient as the test set was iterated 23 times. Both the training and test sets were normalized on each pass using statistics from the training set. Accuracies, sensitivities, specificities, positive and negative predictive values and Cohen's kappa coefficient are averaged across all 23 passes for overall unbiased estimate of performance.

III. Results

Tables III and IV shows the confusion matrix and positive predictivity, negative predictivity, sensitivity and specificity and Cohen's κ coefficient results for a comparison between the automated classification algorithm and the manually annotated data for 5624 breaths. Features selected in order were 18, 20, 19, 11 and 21.

TABLE III. CONFUSION TABLE AND PERFORMANCE RESULTS FOR INEFFECTIVE EFFORTS CLASSIFICATION

		Human Expert System		
		eIE	**Other**	**Total**
Automatic Classifier	**eIE**	333	66	399
	Other	234	4991	5225
	Total	567	5057	5624

TABLE IV. CONFUSION TABLE AND PERFORMANCE RESULTS FOR INEFFECTIVE EFFORTS CLASSIFICATION

Measure	Mean
Positive Predictivity	83.5%
Negative Predictivity	95.5 %
Sensitivity	58.7%
Specificity	98.7%
Cohen's κ coefficient	0.66
Overall Accuracy	94.7 %

IV. Discussion and Conclusions

A non-invasive and simple method for detecting major forms of asynchrony in patient-ventilator interaction has been designed and compared to a human expert-based classification system using a database of 23 subjects.

Overall accuracy (94.7%) and specificity (98.7%) of the classifier is excellent, whereas the sensitivity (58.7%) is moderate. The κ coefficient is a chance-adjusted measure of agreement between two raters [5]. The κ obtained (0.66) represents a good level of agreement between the systems.

Possible causes for the lower sensitivity relate to the fact that timed pressure support breaths were common in the data. In such modes containing these breaths, it is intentional that the ventilator ignores normal efforts exerted by the patient, preferring to dictate the timing in a metronomic fashion. As a result, normal size efforts may influence the flow signal producing normal positive swings that are not accompanied by pressure support. These efforts, while still classed as ineffective, are not the pathological variety that are influenced largely by intrinsic PEEP and hyperinflation and which preoccupy the main concern of clinicians for patients on pressure support ventilation. Pathologic eIEs occur with smaller and negative value flow swings relative to their timed-mode-induced counterparts. As such the combined feature vectors intersect a greater proportion of other breath classes. In future, relabeling of this class as two subsets may improve the sensitivity of the classifier. Another factor influencing the sensitivity is the similar morphology between eIEs and early cycling (another asynchrony type): both are categorized by a perturbation on the flow signal during expiration (and correspondingly on the pressure), however they differ by the elapsed time at which they occur from the start of expiration. This factor is subject dependent, and may be ambiguous even by expert visual inspection.

General factors limiting classifier performance include artifacts such as coughs, swallowing, and abdominal effort, as well as incorrect breath labeling brought about by human error and ambiguity where the Pdi signal is noisy, exhibits large drifts, or where esophageal spasms occur.

In the authors' previous work [6], an online algorithm was developed to detect the presence of asynchrony. Overall performance was very good; however the algorithm contained fixed thresholds and a limited featured set. Also a greater proportion of the eIEs were induced under timed-mode as described above due to low prevalence of those naturally occurring. Thresholds were tuned accordingly.

To the authors' knowledge, only two other attempts to automate detection of eIEs exist. In [2], a 'real' patient effort signal is estimated via optimization of respiratory mechanics measures, and eIEs are detected as an increase of this signal beyond a fixed threshold without an associated ventilator breath. Sensitivity was reported as 79.7%. In [3], a logistic regression classifier is used to determine optimal thresholds for two morphological features. Maximum sensitivity (93.3%) and specificity (92.9%) were high, however as the authors acknowledge, their data did not contain certain artifacts that increase the probability for misclassification. In both studies also, the prevalence of eIEs was much greater than in the current study, and chance adjusted performance analysis would provide a fairer comparison of algorithms.

In conclusion, we show that using a pattern classification approach to automating the detection of eIEs is feasible and with further work to increase the sensitivity of the current algorithm, may provide clinical utility for assessing the quality of patient-ventilator interaction.

V. References

[1] L. Vignaux, F. Vargas, J. Roeseler, D. Tassaux, A. W. Thille, M. P. Kossowsky, L. Brochard, and P. Jolliet, "Patient-ventilator asynchrony during non-invasive ventilation for acute respiratory failure: a multicenter study," *Intensive Care Med*, DOI 10.1007/s00134-009-1416-5 2009.

[2] M. Younes, L. Brochard, S. Grasso, J. Kun, J. Mancebo, M. Ranieri, J. C. Richard, and H. Younes, "A method for monitoring and improving patient: ventilator interaction," *Intensive Care Med*, vol. 33, pp. 1337-46, 2007.

[3] C. W. Chen, W. C. Lin, C. H. Hsu, K. S. Cheng, and C. S. Lo, "Detecting ineffective triggering in the expiratory phase in mechanically ventilated patients based on airway flow and pressure deflection: feasibility of using a computer algorithm," *Crit Care Med*, vol. 36, pp. 455-61, 2008.

[4] P. Pudil, J. Novovicova, and J. Kittler, "Floating search methods in feature selection," *Pattern Recognition Letters*, vol. 15, pp. 1119-1125, 1994.

[5] R. Bakeman and J. M. Gottman, *Observing Interaction: An Introduction to Sequential Analysis*. Cambridge, UK: Cambridge Univ. Press, 1986.

[6] Q. Mulqueeny, P. Ceriana, A. Carlucci, F. Fanfulla, M. Delmastro, and S. Nava, "Automatic detection of ineffective triggering and double triggering during mechanical ventilation," *Intensive Care Med*, vol. 33, pp. 2014-8, 2007.